Particle comminution defines megaflood and superflood energetics

Paul A. Carling, Xuanmei Fan

PII: S0012-8252(19)30564-1

DOI: https://doi.org/10.1016/j.earscirev.2020.103087

Reference: EARTH 103087

To appear in: *Earth-Science Reviews*

Received date: 19 August 2019

Revised date: 1 January 2020

Accepted date: 13 January 2020

Please cite this article as: P.A. Carling and X. Fan, Particle comminution defines megaflood and superflood energetics, *Earth-Science Reviews*(2019), https://doi.org/10.1016/j.earscirev.2020.103087

Particle comminution defines megaflood and superflood energetics

Paul A. Carling[1], Xuanmei Fan[1*]

State Key Laboratory of Geohazard Prevention and Geoenvironment Protection, Chengdu University of Technology, Chengdu, Sichuan 610059, China

*Corresponding author [fxm_cdut@qq.com]

Keywords

Megafloods, communition, flood energetics, streampower.

Abstract

The concept of 'megafloods' and 'superfloods' was introduced at the end of the last century to define exceptionally large-discharge floods, primarily those associated with the failure of Quaternary ice-dams. These floods exceeded, by one or two magnitudes, historically recorded floods, megafloods having peak discharges equalling or exceeding, 1 M m^3s^{-1}. Herein, the sediment associations of exceptional floods are found to be distinctive, being dominated by comminuted (smashed) grain-size distributions, which contrast to the sediment deposits of more moderate floods. A consideration of the energetics of moderate floods, superfloods and megafloods with respect to the entrainment, dis-entrainment, suspension and comminution of coarse gravel allows thresholds of energy expenditure to be proposed that reflect general transformations in flood behaviour that relate to distinctive flood deposits. A threshold of energy expenditure - 20 kJ s^{-1} m^{-2} - is proposed to separate moderate floods from superfloods; the latter by this definition can be ~ 0.1 M m^3s^{-1}. This threshold separates floods competent to entrain cobbles and boulders (with limited comminution of the load) from superfloods that comminute the suspended cobbles and boulders to produce fine granules in suspension. The granules are subsequently deposited to form distinct depositional units that are characteristic of superfloods and megafloods. The energetic threshold is consistent with the lower range of power expenditures associated with the original definition of a megaflood in terms of peak fluid flux.

Significance Statement

Exceptional floods occurred in prehistoric times; the largest are referred to as 'megafloods' or 'superfloods'. To distinguish such exceptional floods from other large floods, megafloods were defined as having a peak discharge exceeding 1 M $m^3 s^{-1}$. However, many reports of 'megafloods' are flows with a peak discharge smaller than 1 M $m^3 s^{-1}$. Recent research has shown that megafloods and superfloods deposit distinctive layers of smashed gravel, which is not the case for smaller floods. The gravel is smashed by exceptionally high-energy expenditures. Consideration of the energetics of floods to transport gravel allows a robust quantitative definition of 'superflood' based on the energy needed to smash a range of gravel sizes.

Key Words

Megafloods, prehistoric floods, comminution, energy expenditure, suspended sediments

1.0 Introduction

In the closing decade of the 20th Century, a variety of terms was used as epithets for unusually large freshwater floods including: cataclysmic flood, catastrophic flood, diluvial flood, extraordinary flood, high-discharge flood; high-energy flood, megaflood and superflood. The adjectives and prefixes were used in a general non-specific sense to distinguish unusually large floods from the scale of floods associated with normal river processes. At the time, the best documented exceptional floods were modern glacial outburst floods (jökulhlaups) in Iceland and ancient examples associated with the Pleistocene Laurentide Ice Sheet and the Channeled Scabland of north-western USA. Although it was recognised that exceptional floods might have long-lasting impacts on landscapes and alluvial stratigraphy beyond those achieved by normal river processes (Baker, 2002; Papp, 2002; Russell, 2005), the issue of defining the qualities of exceptional floods, that might set them apart, remains unresolved (Tómasson, 2002; Marren, 2005; Carrivick and Tweed, 2019).

Baker (1996) used the term 'megaflooding' without definition to describe large-scale Quaternary freshwater flooding. Latterly, Baker (2002) calculated that these exceptional floods had peak discharges (Q_p) estimated to exceed 1 million cubic metres per second (1 Sverdrup) and suggested this discharge quantity as a useful scalar to delimit the magnitude of the largest exceptional floods. More recently, Baker & Carling (2020) have suggested that highly-energetic floods (less than 1 Sverdrup) might be termed 'superfloods', but no defined threshold separates these floods from lesser, moderate floods. Baker (2002) pointed out that exceptional flood freshwater discharges were only high-energy when flowing on steep gradients and, for that condition, were unusually powerful and transformative in terms of the scale and permanence of landscape changes that resulted from erosion and sedimentation during the floods.

Note that Baker (2002) qualified the term megaflood as requiring an adequate gradient to achieve significant work within the landscape. This observation means that the value of 1 Sverdrup is not an energetics threshold value which can definitively separate moderate floods from exceptional floods. Baker and Costa (1987) and Baker (2009) argued that analysis of the palaeohydraulics of these high-energy megafloods demonstrated that they generated unit stream powers in excess of 10^3 W m^{-2} (typically 10^4 to 10^5 W m^{-2}) with bed shear stresses greater than 10^3 N m^{-2}, often reaching 10^4 N m^{-2}.

Reynolds numbers can exceed 10^9, implying exceedingly high levels of turbulent mixing, in such deep and high-velocity floods (Denlinger and O'Connell, 2010; Carling *et al.*, 2010). These values are two orders of magnitude greater than is typical of the world's large rivers in flood and the lower end of the power and stress ranges are equal to the largest recorded values from rainfall-runoff floods and the failure of man-made dams in the USA (Baker and Costa, 1987; Baker, 1996). Although Baker's (2002) definition of a megaflood is precise, publications subsequently often have used the term loosely to define any large flood, many of which have discharges an order of magnitude lower than that of the definition. Since the millennium, the number of published examples of exceptionally-large palaeofloods has burgeoned and it is clear that distinctive sedimentary associations of 'smashed' (*i.e.* comminuted) gravel clasts characterize exceptional floods, primarily as layers of granules deposited from suspension (Carling, 2013a). The 'Udden–Wentworth'' grain-size scale is used to define gravel fractions and classes throughout (Blair and McPherson, 1999).

Consequently, this paper develops a refined definition of the transition from moderate flood to 'superflood' from a consideration of the energy expenditure and associated modes of sediment transport within high-energy floods. The issue arises as to whether the work done, or the landforms produced, by exceptionally-large floods differ(s) from that of lesser floods. Carling *et al.* (2009) considered the issues related to using the associated landforms to define the occurrence of exceptional floods commensurate with the megaflood or superflood appellation, but to date there have been few attempts to relate the energetics of large floods to any distinct suite or scale of landforms (O'Connor, 1993; Benito, 1997; Carrivick, 2007; Carrivick *et al.*, 2013). An alternative approach is to ascertain if megafloods and superfloods produce distinctive stratigraphic and sedimentological signatures (Carling, 2013a) which, if identified in the field, can set them aside from lesser, moderate floods. As noted above, and as detailed latterly, high-energy floods comminute large clasts in suspension. Consequently, it is hypothesized that only floods of a given magnitude will generate sufficient energy to comminute coarse gravel. In this way, megafloods and superfloods might be separated from lesser large floods using the principles of energetics. In Sections 2.0 and 3.0 this concept is elaborated fully.

2.0 Method

A review of relevant literature is used together with a consideration of the theoretical and empirical equations that relate: (1) the entrainment of coarse gravel from an immobile compact or loose bed; (2) the deposition of coarse gravel to form an immobile loose bed; (3) the suspension of coarse gravel, and; (4) the comminution of gravel from large clasts to small clasts as energy is expended to

fracture one or more clasts in mutual collision within a turbulent-suspension of gravel clasts. These various transformations of physical state may be regarded as 'thresholds' and have been defined variously using units of force, stress, power and energy dissipation depending on the approach taken by different authors. Consequently, for the purpose of this study, the energy dissipation associated with each threshold is standardized as kiloJoules per second per metre-squared ($kJ\ s^{-1}m^{-2}$).

Kinetic energy and power

The kinetic energy of water is proportional to the rate of flow. The relationship for the kinetic energy per unit volume of water is thus proportional to its velocity and can be expressed as:

$$E/V = 1/2\rho U^2, \quad (1)$$

where E is the kinetic energy of the fluid in joules (J) per cubic meter, V is the fluid volume (m^3), ρ is the fluid density (kgm^{-3}) and U is the velocity of the fluid ($m\ s^{-1}$). From Eq. 1, the power associated with the kinetic energy can be expressed as:

$$P = 1/2\rho A U^3 \quad (2)$$

where P is the power in Watts per cubic meter ($W\ m^{-3}$) and A is the cross-sectional area of the flow. The result of the cubic relationship is that a flow with twice the velocity of a reference value will have eight times the kinetic energy.

2.1 Initial motion threshold

Whilst acknowledging that exceptional floods might entrain large rocks from fractured bedrock outcrops and talus-covered slopes along the floodway, the entrainment processes of flood-waters in those situations are poorly known. Consequently, below the focus is upon boulder entrainment from alluvial beds. Because of the difficulty of making direct measurements in large discharge fluvial flows, initial entrainment of coarse gravel (*i.e.* medium to very coarse boulders Blair & McPherson, 1999) has not been well-studied except from a theoretical perspective mediated by relatively small-scale experimental data (*e.g.* Carling and Tinkler, 1998; Carling *et al.*, 2002; Lamb *et al.*, 2015). Lamb *et al.* (2015) and van Rijn (2019) indicated that the Shields function (Eq. 3) was appropriate to apply to boulder entrainment and, for the range of coarse gravel grain-sizes, Θ tends to be a constant set equal to an average value of 0.05 or slightly lower (Dey & Ali, 2019), but field and experimental data indicated a minimum range for Θ of 0.02 to 0.025 for more mobile clasts (Dey & Ali, 2019):

$$\theta = \frac{\tau_o}{(\rho_s - \rho)\, gD} \quad . \quad (3)$$

Here, Θ is the Shields number, τ_o is the boundary shear stress, ρ_s is the density of the clasts, g is the acceleration due to gravity and D is a representative size for the clasts. Empirical boulder

entrainment data considered by Costa (1983) consisted of a data compendium of observed boulder movements and calculated bed shear stresses (N m^{-2}) derived for modern flash floods (Komar, 1987). The analysis of Costa supports the use of Eq. 3, as the average value of the Shields parameter (Θ) was 0.04 (s.d. of 0.011 for n = 40) for gravel in the size range 20mm ≤ D ≤ 5000mm. Thus, these empirical data return Θ-values consistent with the theoretical conclusions expressed by Lamb *et al.* (2015), van Rjin (2019) and Dey & Ali (2019) amongst many others, such that the empirical function proposed by Costa:

$$E = 4E\text{-}05D^{1.83} \qquad (\Theta = 0.04) \qquad (4)$$

can be varied, reducing the threshold for entrainment in Eq. 4 from Θ = 0.04 to 0.02, for example, to allow for natural variability in boulder stability, from close-packed (Eq. 4) to looser beds (Eq. 5) respectively.

$$E = 4E\text{-}06D^{1.83} \qquad (\Theta = 0.02) \qquad (5)$$

The variation in the value of Θ, as epitomized in Eqs. 4 and 5, represents a zone of maximum stability (Mantz, 1977) of fairly close-packed clasts, with even lower values (*e.g.* Θ = 0.02 to 0.01; Ramette and Heuzel, 1962; Fahnestock, 1963; Fenton and Abbott, 1977; Church, 1978; Andrews, 1983; Carling, 1983; Hammond *et al.*, 1984) representing very loose beds as explained below.

2.2 Deposition threshold from suspension to a weakly-mobile bed

Deposition is defined herein as the final stage of incorporating a depositing clast to the bed alluvium, which usually occurs from traction. However, the term dis-entrainment also is used herein to emphasize the process complexity whereby sediment particles are released from the flow and come to rest on the bed, the physics of which are not considered here. In lower-energy back-flooded environments, such as embayments, close to the main powerful flood-flow, large clasts can be injected into the backwater firstly as a traction load and latterly clasts can deposited (above the traction deposits) to a rapidly-aggrading bed directly from suspension, often forming giant bars (Carling, 2013a) as well as other outwash deposits (Carrivick *et al.*, 2007). In some instances, as clasts fallout from suspension, a degree of clast reorientation and indeed transport will occur as a short-lived traction load, but the clasts are rapidly immobilized and buried, often resulting in no preferred clast fabric (Carrivick *et al.*, 2004a&b). Surprisingly, there has been little attention given to dis-entrainment processes (O'Connor, 1993) until recently (Dorrell *et al.*, 2018; Leeuw *et al.*, 2019).

Most studies assume that deposition from traction to a static bed will occur in accord with the entrainment threshold defined by Eq. 3; for example, cessation of traction motion occurs when Θ < 0.04 (Pähtz and Durán, 2018); as explained in the next paragraph this may not be the case.

Adopting a threshold Shield's parameter of Θ = 0.045, a near-constant threshold of τ_o = 40–50 N m^{-2} for the cessation of cobble and boulder transport was observed during a series of floods in a bedrock channel (Richardson *et al.*, 2002). In contrast, the thresholds for initial motion was highly variable between flood events at 40–100 N m^{-2}. Temporally-variable thresholds of initial motion also have been reported for alluvial gravel-beds (*e.g.* Garcia *et al.*, 2000) and variation in the critical shear stress for clasts of similar size and shape is attributed largely to packing effects (Brayshaw, 1985; Powell and Ashworth, 1995; Dey & Ali, 2019). The difference between critical shear stresses for initial and final motion recorded by Richardson *et al.*, (2002) also has been observed for alluvial gravel-beds (Reid *et al.,* 1985) where the difference in entrainment and dis-entrainment was on average a factor of 3. Hjulström (1935) and Sundborg (1956) similarly reported the difference in entrainment and dis-entrainment velocities as being a factor of 1.5 to 2. The difference, in part, can be explained by the 'under-loose' condition of groups of depositing clasts, in contrast to the close-packing of clasts within a bed at initial entrainment, which allows transport to continue for lower values of the critical shear stress on the waning limb of a flood.

In the case of suspended clasts, there is little information on dis-entrainment in contrast to suspension thresholds which are well researched. The Izbash function (1935; Izbash and Khaldre, 1970) underpins several modern engineering approaches to determining the stability of blockstone dumped at the water surface to settle to a static or weakly mobile bed (Langmaak, 2013; Langmaak and Basson, 2015) and so is applied here to boulders deposited from an exceptional flood. As reported by Carling and Tinkler (1998), the function determines the critical near-bed velocity (U_c) for stability of isolated, or close-packed boulders:

$$U_c = \sqrt{\frac{2Dg}{C_1(\rho/\rho_s - \rho)}}, \quad (6)$$

where C_1 is a packing coefficient: 1.35 for isolated (underloose) boulders. The bed shear velocity (and subsequently the bed shear stress) is estimated from the predicted U_c value utilizing the general velocity profile function (Schlichting and Gersten, 2000):

$$U_c/u_* = 1/k \ln z/z_o, \quad (7)$$

in which *k* is the von Kármán constant (0.4), *z* is the height above the bed and z_o is a bed roughness value.

At the simplest, the modes of suspended sediment transport - partial through to full suspension - may be distinguished by a ratio of the settling velocity of the particle in still water to the flow frictional shear velocity (a proxy for the turbulence acting to suspend particles):

$$R_o = W_s/kU_* \quad (8)$$

where R_o is the Rouse number, *k* is the von Kármán constant, (usually about 0.4, although *k* values in the range 0.12 to 0.65 have been reported), W_s is the settling velocity and U_* is the frictional shear velocity that is proportional to the bed shear stress, $U_* = \sqrt{\tau_o/\rho}$. Generally, when R_o is in the range 1.2 to 2.5, 50% of the bed material will be suspended, whereas for R_o in the range 0.8 to 1.2 100% will be in suspension (*e.g.* Valentine, 1987).

Sadat-Helbar *et al.*, (2009) reviewed 22 published settling velocity relationships and the data for clasts up to 100mm in size. Their revised settling relationship is described in terms of a Particle Reynolds number (*Re*) and effective non-dimensional diameter (D_{gr}):

$$R_e = \frac{W_s D}{\upsilon}$$

and,

$$D_{gr} = D\left(\frac{g(s-1)}{\upsilon^2}\right)^{1/3}$$

yielding for gravel clasts > 40mm;

$$W_s = 0.51\frac{\upsilon}{D}\left(\frac{D^3 g(\rho_s-\rho)}{\upsilon^2}\right)^{0.533} \quad (9)$$

For example, equation 9 returns a settling velocity of 2.36 ms^{-1} for a 100mm sized clast, so with reference to Eq. 9 and setting R_o = 2.2 and *k* = 0.4, a near-bed shear velocity of 2.33ms^{-1} indicates that 100mm clasts, within a broader mix of clasts sizes, are at threshold for settling to the bed.

3.0 Context and Results

3.1 Comminution of clasts in traction and in suspension

Comminution of rock in water flows is predominantly due to attrition (disintegration) of the rock-bed surface or of particles in transport (Whipple *et al.*, 2000). In the case of discrete particles,

attrition refers to a reduction in the strength of a clast through sustained stressing of the particle. The results of attrition usually are referred to as abrasion and fracturing (Attal and Lavé, 2009).

Abrasion is evident largely as chipping, scratching and polishing of the clast surface caused mainly by shear at the particle surface (Ghadiri and Zhang, 2002), whereas 'fracture' is used herein to mean breaking a clast into two or more large fragments (Chen *et al.*, 2007), rather than removing a small chip from the surface of a clast. Abrasion is a localized low-energy stressing of particles, predominately affecting those stronger particles in prolonged contact in traction (Kodama, 1994a and b), whereas fracturing in traction largely effects *weak* lithologies (Adams, 1979). In contrast, fracturing of *weak* and *strong* lithologies (the strength classification used is that of the British Standards, 1981), occurs due to high-energy impacts, primarily clast-to-clast interactions in suspension (Campbell, 1963; Wohletz *et al.*, 1999), wherein abrasion is less important. Usually it is assumed that the collision properties due to impacts between clasts and the boundary and between individual clasts in suspension are the same (Foerster *et al.*, 1994). The greater the fracture surface energy applied in the fracturing process, the smaller the residual clast size (Kusnetsov, 1973). However, the final clast size is mediated by the structural characteristics of the rock-type, as well as by the duration over which the energy is applied to the population of clasts (Adams, 1979; Chen *et al.*, 2007). Further, as the particle size is reduced, liquid drag on suspended clasts becomes increasingly dominant so that small particles more completely conform to the movement of the fluid (Richardson & Carling, 2005) and the velocity of impacts tends to decline so fracturing tends not to occur below a clast size-threshold.

From the above, although fracture surface energy can be calculated theoretically and measured by careful fracture experiments (Ball and Payne, 1976), the irregularity of natural clasts and the complexity of particle interactions (Labous *et al.*, 1997; Hurley *et al.*, 2018) due to shape and the presence of flaws in the clasts, for example, means that no generalized solution is available relevant to this application, although Kick's law, detailed below, provides a useful framework. For dry rocks, fracture surface energy can be as low as 7-200 $Js^{-1}m^{-2}$ (Friedman *et al*, 1972; Chelidze *et al*, 1994; Ouchterlony, 1982) and the fracture surface energy increases linearly for small near-homogeneous particles as rock sizes increases to around 58mm in diameter. Above 58mm a significant linear reduction in strength occurs, due to the increasing number and size of flaws found in larger rocks (Hoek and Brown, 1980; Hawkins, 1998), yielding a shallow inverted V-shaped curve from granules to coarse cobbles. The issue of appropriate energy expenditures within exceptional floods is revisited more fully in the sections below.

3.2 Comminution of Suspended Rock Debris in Large Floods

Given the high stream powers associated with large floods, boulders can be mobilized in traction or suspended and large sediment loads are possible (O'Connor, 1993). For example, modern jökulhlaups typically develop sustained power of around 3000 to 5000Wm^{-2} (Carrivick, 2007; bed shear stresses ~ 4000 - 8000 Nm^{-2}; Carrivick *et al*., 2013) which specific values entrain 465mm to 610mm clasts (Costa, 1983) and, with reference to Eq. 6 (see Method), suspend 100 to 200 mm sized clasts (Russell and Knudsen, 1999), whereas short duration peak flows can be associated with power expenditure of 40,000 W m^{-2} which can suspend 2m boulders (Russell, 2005). In comparison, power values of 10^5 to 10^6 Wm^{-2} were generated for the largest Quaternary floods, sustained over large distances and for durations of several days. These Quaternary floods suspended large blocks but also comminuted rock debris to produce fine suspended granules that are observed in exceptional flood deposits worldwide (Carling, 2013a; see also Fig. 2). These high-energy gravel-transport processes are unusual in modern depositional settings, such that most investigators assume coarse gravel always is deposited from traction and not from high-concentration suspensions (Shanmugam, 1997). Nonetheless, with exceptional flood dynamics when interpreting the origin of gravel beds, it is not possible to preclude the possibility of deposition of gravel from high-concentration suspensions (Lord and Kehew, 1987; Mutti *et al*., 1996).

It was J Harlen Bretz (1929) who first noted the abundance of broken gravel clasts in the basal planar bedded or clinoform coarse-gravels (megaflood sequences 1 & 2 of Carling, 2013a) and the overlying laminated fine-gravels (megaflood sequence 3 of Carling, 2013a) composing giant bar deposits of the Washington scablands. Bretz (1929) contrasted this abundance to a much lower frequency of fractured clasts in the neighbouring modern Snake River wherein most clasts were well-rounded. The giant bar gravels consisted primarily of basalt, but also contained diorite, porphorytic lava, quartzite and schist. Large boulders were few (<0.60m in diameter) with 75 to 96% of cobbles and pebbles smashed and exhibiting ragged fractures. Some 50% of coarse sand grains were also smashed and angular. Bretz concluded that a high-velocity flood, over 100m deep and capable of tearing rock from the valley sidewalls, transported, fractured and thus comminuted the large boulders due to percussion. However, he argued that the high preservation of ragged fractures indicated that subsequent deposition and burial must have been rapid.

The observations of Bretz (1929) demonstrate remarkable insight and provide a spur to define the scale of exceptional flooding from a consideration of flood energetics. As was proposed in the

Introduction, only floods of a given magnitude will generate sufficient energy to comminute coarse gravel, reducing large clasts to fairly uniformly-sized grains; typically of granule size (Carling, 2013a). Although the detail of size-reduction processes is lacking, many exceptional flood deposits consist of mixtures of granules derived from incompetent lithologies with less frequent boulders composed of competent lithologies (Carrivick *et al.*, 2004a&b). In this way, a distinction might be drawn between the energy expended by 'normal' moderate flood action and the expenditure of superfloods; thus providing a physical basis for the definition of a superflood. As there are no data related to comminution of rock debris during natural large floods, indication of the process can be derived from published laboratory investigations of rock fracture and resultant grainsize distributions.

There is little information on the fragmentation processes due to suspended rock-particle collisions in experimental water flows. Nevertheless, the fracturing kinetic energy is derived from the strain energy released at failure. The energy required to break intermolecular bonds and form new surface area due to the fracturing process is the fracture surface energy; this is commonly set equal to the failure strength of the clast (Pittman and Ovenshine, 1968). Walker *et al.*, (1937) proposed that the energy:particle-communition size relationship was of the form:

$$dE = -C\frac{dD}{D^n}, \tag{10}$$

where E is the net specific energy required to comminute a given clast size (D) and C is a constant. This function states that the required energy for a differential decrease in size is proportional to the size change (dD) and inversely proportional to the initial clast size to some power, n. Hukki (1962) demonstrated that the exponent n is size-dependent. When the exponent is equal to 1, then the function reduces to Kick's law, applicable to fracturing, whereas when the exponent is 2, the function applies to abrasion, but to a narrow range of sizes ($D \leq 50$mm) in both instances. Kick's law states that if a given specific energy is required to fracture a clast of size D, a clast half that size will require half the energy expenditure (Hukki, 1962). Grain-size distributions of comminuted clasts due to fracture plot as single-population linear functions on ln-ln coordinates (*e.g*. Genc and Benzer, 2009; Tuzcu and Rajamani, 2011; Xu and Wang, 2017). This comminution distribution is known as the Gates-Gaudin-Schuhmann (GGS) function (*e.g.* Gupta and Yan, 2016; Petrakis *et al.*, 2017) and examples for industrially-crushed rock are shown in Fig. 1. Also shown in Fig. 1A are bedload gravel size-distributions of deposits produced by an exceptional but otherwise 'normal' moderate river flood. Within plots of the form shown in Fig. 1A, natural flood gravel samples commonly plot as two populations, one fine and one coarse, separated by an inflection point, in this case between 20mm and 8mm (arrowed in Fig. 1A). The finer population is small and is sourced from suspension-settling and tends to be quasi-linear whereas there is a tendency for the coarser traction-deposited

population to be convex upwards, in distinct contrast to the crushed rock samples. Thus, these moderate-flood samples do not plot as GGS-distributions. In contrast, an exceptional high-energy flood from a landslide dam failure produced grain-size distributions of fine comminuted gravel very similar to laboratory crushed rock samples (Fig. 1B).

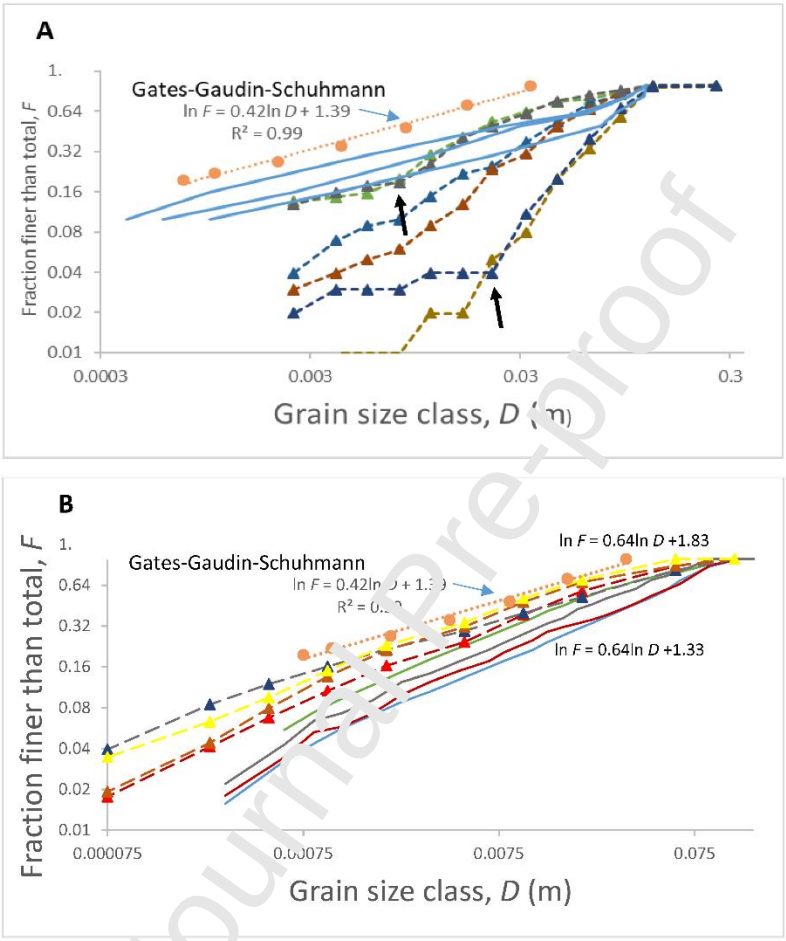

Fig. 1: *The Gates-Guadin-Schuhmann grainsize distribution function: (A) Samples of laboratory crushed rock (Gupta and Yan, 2016; orange dots; orange ln-ln function shown (blue arrow)) and (Schendel et al., 2014; solid blue lines, seven data points per sample). Triangles represent water-transported bedload deposits in the Rivers Cocker and Derwent (resultant upon the 2009 >1:500 year recurrence flood, e.g. Q_p c. 395m^3 s^{-1} in the Derwent; Chiverrell et al., 2019) in the English Lake District (ELD). (B) Samples of laboratory crushed rock (Gupta and Yan, 2016; orange dots; orange ln-ln function shown (blue arrow)) and (Kim, 2010; four solid lines, 26 data points per sample; ln-ln distributions are shown for green and blue data sets). Triangles represent water-transported comminuted gravel samples from the Yigong River landslide dam-break flood (Shang et al., 2003).*

3.3 Stratification Styles and Grain-size Distributions in Exceptional Floods

Distinct coarse-fine layering of gravel beds (Fig. 2A), scour and fill structures and cross-bedding, commonly develops in the usual annual floods in fluvial systems due to selective entrainment within under-capacity flows, where the rates of traction transport of coarser clasts is low and deposition directly from suspension is negligible. Clasts in traction tend to be abraded, rather than fractured, and consequently assume characteristic ellipsoidal shapes (Koster *et al.*, 1980). Such processes are mediated by fluctuations in discharge that result in periods of low-transport rates that further winnow the depositing surfaces. Thus, low-energy expenditure is associated with defined stratification, as clasts have time to orientate with the flow before burial (Malde, 1968; Rust, 1972; 1977). Thus, prolonged shallowing flows may be associated with stronger clast fabrics (Maizels, 1993; Lønne, 1997; Russell and Marren, 1999; Cutler et al., 2002).

In contrast, with regard to high-energy floods, very-coarse sediment such a cobbles and boulders can form parallel bedding or low-angle clinoforms when deposited rapidly from traction, but stratification can be diffuse as particles did not have time to fully-orientate with the flow before rapid burial (Carling, 2013a; Fig. 2B). These styles of coarser-grained bedding primarily occur on the rising stage of a flood in backwater locations as described below, but less commonly may occur on the waning limb of a flood. The rising stage clinoforms in turn are capped by finer, horizontally-bedded sediments with poorly-defined lamination (Fig. 2C), probably deposited from suspension (Carling, 2013a). These particles are dominated by fractured and have slightly-rounded angular clast shapes (Fig. 2D), as was first noted by Bretz (1929) as well as by numerous authors subsequently (*e.g.* Norris *et al.*, 2019); as described below.

High-energy modern moderate floods regress steadily, but rapidly, and have near-capacity loads including high suspended sediment concentrations which, upon deposition, lead to beds in which distinct layering tends to be absent due to intense deposition rates (Laronne *et al.*, 1994). Fine sediment, such as fine sand, silt and clay is notable in its absence having been winnowed from depositing beds and transported down system (Carling, 2013a). Similarly, within prehistoric exceptional floods, settling from high-concentration suspensions largely resulted in rapidly aggrading, diffuse bedding that is largely fines-free. Particle-orientation often is weak (Carling, 2013a), as is typical of gravity-dominated fabrics (Dapples & Rominger, 1945; Allen, 1982, p. 189). Nonetheless, a degree of size-segregation may be evident due to turbulence mediating variations in the applied fluid shear at the bed producing graded deposits (Carling, 2013a). Such ill-defined lamination of coarse-sediments in modern shallow rivers most commonly is associated with rapid deposition to upper-stage plane beds within supercritical flow. However, exceptional floods (despite their high

velocities) were exceeding deep and consequently mean Froude numbers often were sub-critical (*e.g.* Carling *et al.*, 2010; Winsemann and Lang, 2020; Carrivick *et al.*, 2013; Benito and Thorndycraft, 2019), especially in backwaters, largely precluding upper-stage plane beds. Thus, although some flood lamination might be upper-stage plane beds produced in shallow flows, in the majority of cases the lamination is due to the intense deposition to lower-stage plane beds in deep water (Dam, 2002; Carling, 2013a). Indeed, massive and laminated sand deposits (similar to the coarser-grained megaflood laminated sequences) have been produced experimentally from suspension-dominated fallout with negligible shear-flow (Amy *et al.*, 2006).

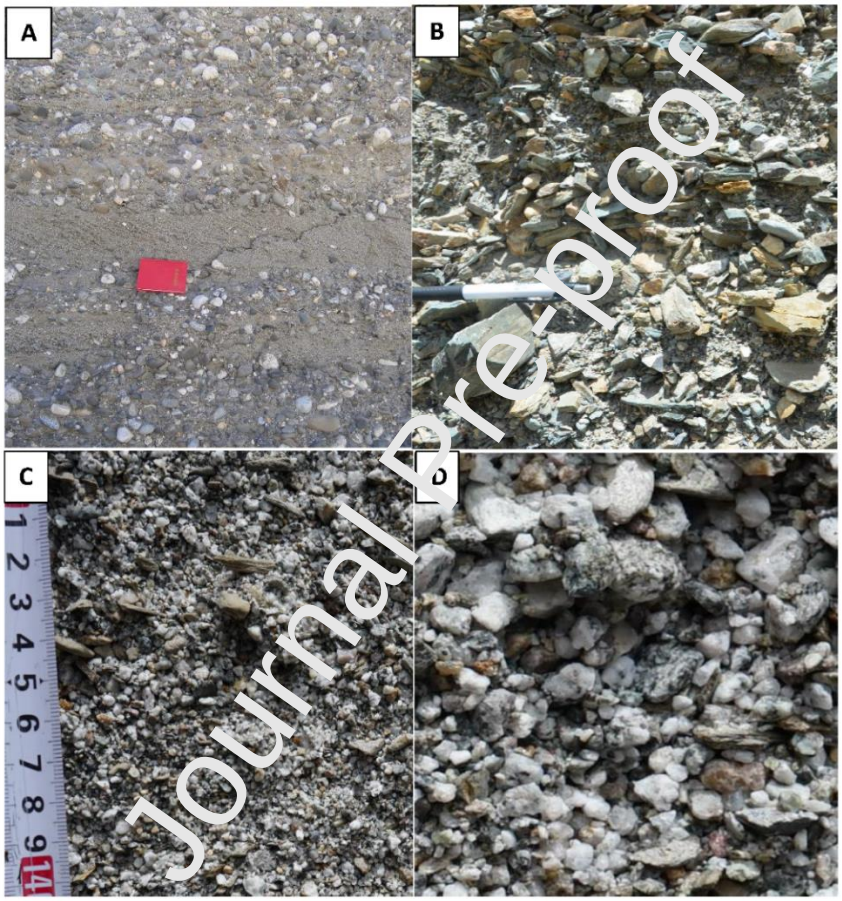

Figure 2: *Variation in bedding styles and particle angularity: A) Layered 'normal' flood well-rounded gravel clasts interbedded with sand beds; B) Angular, coarse, comminuted exceptional flood deposit; B) Angular, comminuted granule-sized exceptional flood deposit; D) Zoom of panel C. Note poor rounding of smashed grains.*

3.4 The Energetics of Rock Debris in High-energy Suspension

In comminution experiments, Lim *et al.*, (2004) observed a lower limit to clast strength attributed to the existence of a minimum structural control on the strength of the clasts, as was noted above. It was proposed that clasts that survive the comminution process are the statistically stronger ones

(Tavares and King, 1998). This supposition is also the case for fluvial pebbles, because the disaggregation of some clasts due to stream transportation leads to a statistical strength increase in the population of clasts (Moss, 1972). Thus in high-energy floods, coarse rock debris in traction and in suspension should be reduced in size to form narrow size distributions mediated by the fracture characteristics of the lithologies present. Although fluid stressing alone may break weak clasts, the size reduction in suspension must be induced primarily by clasts impacting each other within the turbulent flows.

As well as due to the impact force of two clasts colliding, or a clast impacting the boundary of the channel, fracturing of clasts also is controlled by the shape, hardness and structural attributes of different lithologies (Cho & Austin, 2003), as well as the effects of weathering (Bradley, 1970). In contrast to dry impacts, the energy required for fracturing also may be reduced in water (Wills and Napier-Munn, 2006; possibly up to 30%, Hawkins, 1998). Given these controls on fracturing, a wide range of values of impact energy expenditure might be expected to have been responsible for producing any set of fractured clasts of a given grain-size range, especially if mixed lithologies are considered.

Two clasts in collision within a suspension are likely to impact at two singular points (Stronge, 2000) so that the most appropriate laboratory test to determine the energy expenditure at fracture is the point load test (PLT) (Bieniawaski, 1975; Franklin, 1985) which is widely used to determine the tensile strength of both hard and soft rocks (Heidari *et al.*, 2012). Such tests can be performed on individual water-worn clasts, or on rock fragments including core sections. Clearly, the former data are of particular interest within the context of this study, but there are no data for fluvial clasts larger than 20mm. In geotechnical tests of rock tensile strength, cores are taken from large rocks, or from outcrop, and the test results are standardized to represent a 50mm diameter core sample. Thus, field sampling preferentially is focussed on the recovery of near-50mm diameter samples, with few cores or blocks greater than 50mm being tested.

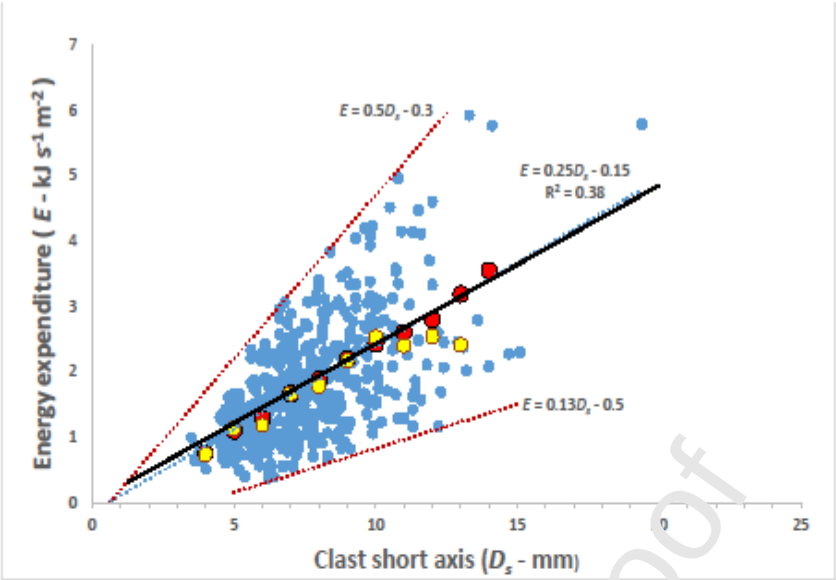

Figure 3: *Variation in experimentally-derived energy expenditures recorded using PLT to fracture pebbles. Red points are 1mm-increment class mean values and yellow points are the median values for those classes where there are sufficient data. Data of Tuitz et al. (2012). Blue dotted curve is the least-squares fit to all blue-dot data (n = 466); the p-value is < 0.0001 which indicates that the regression is statistically significant. Red dotted lines are the lower and upper eye-fitted limits to data spread. Black solid curve is Eq. 1 with n = 1 and C = 1 for Kick's Law. See text for detail.*

Figure 3 provides an example of the PLT experimentally-derived loads needed to fracture samples of natural water-worn ellipsoidal fluvial pebbles composed primarily of limestone clasts (*c*. 90%) but also containing dolomite, sandstone and quartz clasts (*c*. 10%). The specific clast lithologies in Fig 3 do not group by energy expenditure so individual lithologies are not differentiated in Fig. 3. Nevertheless, the least-squares mean trend (blue dotted curve) conforms to Kick's Law: Eq. 1 and the clast size-distribution accords with the Gates-Gaudin-Schuhmann relationship for idealized comminuted particles with a slope $m = 1.02 \approx 1.0$ (Fig. 1). The mean trend and the eye-fitted lower bound (red dotted line) to the data delimit the *weaker* clasts whilst the eye-fitted upper bound (red dotted line) pertains to the rarer, *strong* clasts. This supposition takes no account of the shape and structural attributes of the clasts (as is noted above) which will also have contributed to the data spread in Fig. 3. In addition, the different loading configurations experienced by impacting clasts in turbulent transport will contribute to data spread in similar distributions of the required load. Nevertheless, Fig. 3 indicates a linear positive trend of the required load as a function of increasing grain size for a narrow range of grain sizes. The linear trend is explained as, for small clasts (< 58mm), the larger the clast and therefore the longer the loading axis in the experiment and thus the

higher the resistance of the clast to fracture (Hiramatsu and Oka, 1966). Such a linear trend pertains primarily to populations of clasts that exhibit a fairly-homogeneous microstructure with few defects. Note however that although the mean and median are effectively coincident for smaller clasts, as clast size increases the distributions for each size class becomes right-skewed, suggesting a growing number of weaker clasts in the coarser fractions, as expected for larger clasts. Thus the linear trend is unlikely to pertain to larger clasts (such as cobbles and boulders), as it is generally agreed that there is a significant reduction in strength with increasing rock size above 58mm (Hoek and Brown, 1980; Hawkins, 1998). Although a boulder may not fracture across the full diameter, it will contain more incipient fractures than a cobble of the same lithology and consequently should reduce in size by spalling (Hardin, 1985; Lade *et al.*, 1996). Thus, the mean positive trend in Fig. 3 should transition to a negative trend as grain size increases into the cobble and boulder size-ranges.

3.5 A Definition of Superflood from Energetic Principles

Our stated goal is to define the transition from moderate flood to 'superflood' in terms of the energy expenditure and associated modes of sediment transport within high-energy floods. In the text below, we explain how we construct energy expenditure threshold curves for a range of particle sizes from fine to very coarse gravel (Fig.4A). We define threshold curves for particle comminution of both weak and strong clasts in suspension and refer to a general threshold suspension curve. The conditions for entrainment of bed material into traction from under-loose and loose beds is also considered, as is the issue of dis-entrainment. Dis-entrainment is the condition when clasts are released from the flow, often initially from suspension, rather than from traction, to be included within the deposited bed material. Because there is a lot of information in Fig. 4A, we simplify the diagram within Fig. 4B.

Figure 4 reproduces the trends of the minimum (Curve A), mean (Curve B) and maximum values of energy expenditure (Curve C) required to fracture natural particles in the range 2mm to 20mm as demonstrated in Fig. 3. Also included in Fig. 4A are data for 50mm diameter meta-sedimentary rock cores (Li *et al.*, 2013) which are *extremely-strong* according to the British Standards (1981) classification; the plotting positions of which data concur with a limited extrapolation of the Curve C. A *weak* rock gypsum (Heidari *et al.*, 2012) and a range of rock types from *weak* travertine to a *very strong* granite (Kahraman *et al.*, 2005) are also included. Curves A through C are extrapolated to a value of 50mm. Although such extrapolation possibly is unwarranted, the extended curves from D = 20mm to 50mm serve to indicate the mean and maximum values of energy expenditure that might be required to fracture cobbles into two or more large fragments. The grey curve is the proposed

reduction in energy required as rock sample size is increased from 50 to 200mm (Hoek and Brown, 1980). Taken together, Curve C and the grey curve produce a shallow inverted V-shaped trend centred on D = 50mm, which function was supported by analysis of rock samples of varying strength ranging from 12.5mm to 150mm in size which similarly produce broad shallow inverted V-shaped curves (Hawkins, 1998). Boulders and other larger rock masses can be subject to abrasive comminution (whereby small chips are spalled from the exposed surfaces due to abrasion in traction or by ballistic impacts) for values of energy expenditure (*e.g.* < 10 to 16 kJ $s^{-1}m^{-2}$; Carling, 2013b) that are less than that depicted by positive extrapolation of Curve C to boulder-sized clasts. Consequently, it is evident that the negative trend afforded Curve C through the grey curve, likely delimits an upper limit to the probable energy required to comminute boulder surfaces, above which total boulder fracture becomes increasingly probable as boulders go into suspension. Thus *moderately strong* (e.g. quartzite) boulder comminution should occur for values lower than the grey-curve extension to Curve C and weaker rocks below a similar extension to Curve A (not shown). Note also that the grey curve trends to intersect an extension of the Sadat-Helbar *et al.* (2009) cobble suspension curve (Equation 9) and the Russell (2005) boulder suspension estimates.

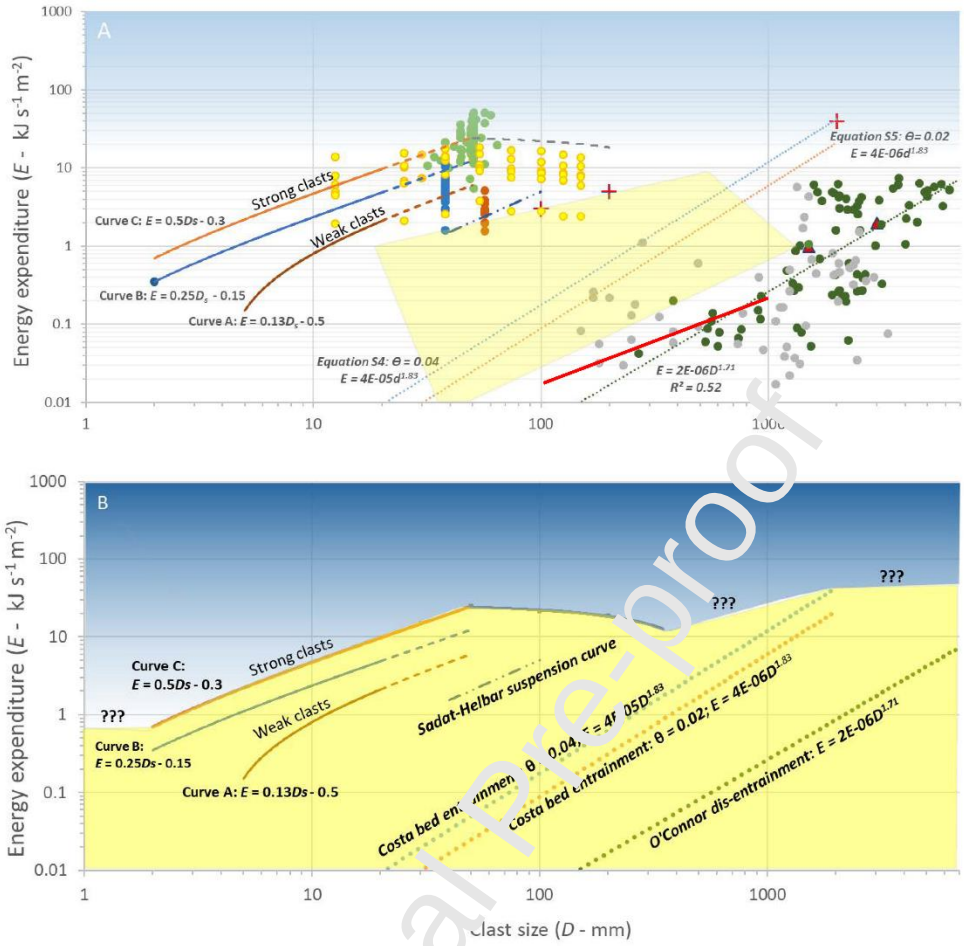

Fig. 4: A: *Energy expenditure related to different clast transport modes within floods (see text for detail). Symbols and curves are defined below from left to right. Curve A, B and C are the minimum (brown), average (blue) and maximum (orange) curves to comminute limestone and quartzite pebbles (< 20mm; see Fig. 3). The maximum Curve C is extended as the grey dashed curve to 200mm after Hoek and Brown (1980). Green symbols represent moderately-hard metasandstones (Li et al., 2013). Blue symbols represent a range of rock types from moderately-soft to moderately-hard (Kahraman et al., 2005). Brown symbols represent a moderately-soft rock: gypsum (Heidari et al., 2012). Yellow symbols represent various sandstones and limestones, with the lowest yellow symbols representing a moderately-soft oolithic limestone (Hawkins, 1998); fitted assuming the unconfined compressive strength (UCS) = kPLT where k is 10 for brittle rocks and 5 for the oolite (Singh et al., 2012) . Blue dot-dash line represents suspension threshold for 4mm to 100mm gravel (Eq. 9; after*

Sadat-Helbar et al., 2009). Red crosses represent suspension threshold for boulders (Russell, 2005). Blue and red dotted lines are threshold for entrainment of boulders with Shields Θ set to 0.04 or 0.02 (Costa, 1983). Red triangles are examples of observed threshold for boulder entrainment (Williams, 1983); yellow area is zone of potential uncertainty for boulder entrainment (Williams, 1983). Green and grey symbols and green dotted trendline represent the threshold for boulder dis-entrainment in the Bonneville flood (O'Connor, 1993); red solid line represents Eq. 6.

B: *Highly-generalized version of panel A. Blue zone is subject to intense comminution processes typically associated with particles suspended within exceptional floods. Yellow zone is subject to processes associated with exchange of particles to and from the bed (i.e. traction dominated) in moderate floods. The lower stages of exceptional floods are also characterised by the energy levels within the yellow zone. Note the shallow inverted V-shaped curve that defines the two zones for a grain size range of c. 10mm to 300mm. The position of extensions to the V-curve (marked by question marks) is uncertain for the range of grain-sizes representing granules and boulders.*

Close-packed boulder entrainment is reasonably well-defined by the Costa (1983) entrainment function (Eq. 4), whereas the Williams (1983) range of uncertainty for gravel entrainment spans initial motion for loose-bed conditions, through close-pack to entrainment into suspension. Uncertainty in the initial motion threshold is largely due mainly to local variation in degree of particle packing, notably particle protrusion above the bed (Komar & Carling, 1991), such that some coarse clasts are entrained for values of Θ = 0.04 in accord with Costa (1983) or for low values of Θ = 0.02 to 0.01 for under-loose clasts, including in catastrophic palaeofloods (Wolman and Eiler, 1958; Bradley and Mears, 1980). Such variability can lead to reports of boulder motion that span the range of uncertainty in Θ-values (e.g. Fort et al., 2010). Fort *et al*. (2010) calculated the entrainment conditions for a range of observed boulder movements subsequent to a Himalayan dam-break flood. For their data (100mm ≤ D_{90} ≤ 4300mm), the empirical function $E = 0.0204 D_{90}^{0.54}$ spans the range from Θ = 0.04 for close-packed 100mm gravel clasts to lower Θ-values for protruding large boulders (4000mm).

Reducing *Θ* within the Costa function to 0.02 (see Method), provides a reasonable upper limit to the data range for deposited boulders reported by O'Connor (1993) indicating that only a few of O'Connor's boulders represent packing configurations close to incipient motion. This last point is important, as the data of O'Connor (1993) represent boulders deposited by the exceptionally large Bonneville flood (peak estimated discharge mostly in the range 0.8 to 1 M m^3s^{-1}) and so termed a megaflood by Baker's definition. For each boulder location, the *minimum* hydraulic conditions for deposition of the boulders was ascertained by O'Connor (1993) using step-backwater modelling of

the individual flood reaches. It is evident that although peak energy expenditure reached 100 kJ $s^{-1}m^{-2}$ (O'Connor, 1993; p 55), final boulder deposition was associated with energy expenditure less than 8 kJ $s^{-1}m^{-2}$. The full Bonneville data set is represented by the grey and green symbols and an empirical least-squares regression for the data from Swan Falls and Hagerman reaches roughly parallels the function proposed by Costa (1983) for entrainment. There is evidently a distinct reduction in the values of energy expenditure at the time of dis-entrainment of boulders in contrast to the energy expenditure associated with initial entrainment. The Izbash (1932; Izbash and Khaldre, 1970) boulder dis-entrainment function (Eq. 6), developed for engineering applications, applies reasonably well to the Bonneville data set (150mm ≤ *D* ≤ 3000mm), if $U_c/u_* = 11$, *i.e*. the height above the bed to the bed roughness, z/z_o = 100 in Eq. 6. A value of $U_c/u_* = 11$ is reasonable, being typical of experimental high-energy turbid flows with similar z/z_o ratios (Sequeiros *et al.*, 2010; their fig. 13). Such a result may indicate that boulders fall rapidly from suspension in deep water to rest loosely on the bed with little time spent in traction. Published engineering solutions to boulder stability might be considered further with respect to defining the deposition threshold for large boulders in exceptional floods, but such a consideration goes beyond the scope of this paper.

To conclude this section, Fig 4B is a generalized version of Fig. 4A. The blue zone in Fig 4b is subject to intense comminution processes typically associated with particles suspended within exceptional floods, which here can be termed 'superfloods'. The yellow zone is subject to processes associated with exchange of particles to and from the bed (i.e. traction dominated) in more moderate floods. The lower stages of exceptional floods are also characterised by the energy levels within the yellow zone.

4.0 Discussion and Conclusions

Although Baker defined a megaflood as having a peak discharge equal to, or in excess of, 1 million $m^3 s^{-1}$, the peak discharge is not sustained through time, so it might be more appropriate to integrate the discharge below the hydrograph and to consider the shape of the hydrograph with respect to the power generated, the energy expended and the potential work done. Sometimes, for moderate floods it has been recommended to integrate the discharge, or the power, above a given threshold discharge Q_c throughout a flood as a measure of the energy available to accomplish work (*e.g*., Costa and O'Connor, 1995; Darby *et al.*, 2010). However, as significant and characteristic coarse gravel deposition occurs for low values of energy expenditure (*c.* 0.1 kJ $s^{-1}m^{-2}$; O'Connor, 1993,) building distinctive horizontal cobble or boulder strata or clinoforms (Carling, 2013a), there is no argument to identify a particular low critical discharge. Rather, a characteristic of exceptional flood hydrographs

is that they tend to be singular events with rapidly waxing and waning limbs and a distinct peak discharge.

Thus, often consideration of the peak discharge value provides just as good an empirical index of the ability of a flood to do sedimentological and geomorphological work as consideration of an integrated discharge above a threshold, or consideration of integrated power. That being said, often flood duration is important mediating such responses as the distance of boulder transport and the degree of bedrock incision. Consequently, as numerical simulations of exceptional flood stratification become more sophisticated the variability of energy expended during the passage of a flood wave could be incorporated into the modelling procedure. More sophisticated modelling of the mechanisms of sediment transport including boulder dynamics, abrasion, and comminution are required throughout flood hydrographs of different peak discharges and durations (Carrivick *et al.*, 2013). In particular, improved understanding of dis-entrainment will help explain the variable character of exceptional flood deposits, not least due to the differential sorting of coarse and fine sediment during the passage of a flood (Carrivick *et al.*, 2011).

In respect of the comments above, and with reference to Fig. 4, as discharge increases and energy expenditure increases, transformations occur in the nature of the sediment transport, which might usefully be termed changes in flood effectiveness that will influence the subsequent depositional sedimentary signatures. Thus, if the definition of a superflood is based on the ability of the flow to comminute gravel in suspension then clearly the threshold for suspension (Fig. 4A) must be exceeded. Above this threshold comminution is defined by nested shallow inverted V-shaped curves, as exemplified by the strong and weak clast curves (Fig. 4A). Thus, strictly speaking defining a superflood in terms of the energetics to comminute gravel is a variable function of both grain-size and the strength of the lithology of clasts in suspension. For example, for an energy expenditure of around 1 kJ $s^{-1}m^{-2}$, small pebbles can be suspended but significant comminution is unlikely, except for very weak lithologies. For an energy expenditure of 10 kJ $s^{-1}m^{2}$, 400mm boulders can be suspended, and comminution will occur for most grainsizes and for *moderately-strong* lithologies. For an energy expenditure of 20 kJ $s^{-1}m^{-2}$, 50 to 1000mm boulders can be entrained and comminution will be universal. The Yigong dambreak (Shang *et al.*, 2003) peak discharge was 'only' 134,558 m^3s^{-1} but produced a peak energy expenditure of around 98kJ $s^{-1}m^{-2}$ at the sediment sampling site for the flood grain size distributions in Fig. 1B. These grain size data consist of comminuted angular fragments coarser and finer than 50mm. So, with reference to Fig 4A there was more than sufficient energy to comminute large clasts to produce the fine grain size distributions. Thus selecting a general threshold of 20 kJ $s^{-1}m^{-2}$ as the defining energy expenditure

separating 'normal' floods from superfloods is consistent with the original definition of an exceptional flood in terms of unit stream power (Baker, 2002) but not necessarily flood peak discharge.

Such a scaled approach to defining flood effectiveness, allows an appreciation to be developed as to the likely effect on sediment transport, grainsize fractionation and deposition, where the flood peak discharge or changes in the hydrograph are known. The corollary is that the sedimentary associations and the degree of particle comminution can be used to infer the energy expenditure (Fig. 4) of a given flood where there is no flood simulation available. Fig. 4B is a highly-generalized version of Fig. 4A delimiting a blue-zone subject to intense comminution processes within exceptional floods. Similarly the yellow-zone is subject largely to fraction dominated processes within moderate floods or the lower stages of exceptional floods. Beyond generalization from Fig. 4B, theoretical consideration and detailed experimental and numerical-modelling work are needed to determine the energy expenditure required to produce well-recorded grainsize distributions (*cf* Austin, 2002) and stratigraphies associated with megafloods and superfloods.

5.0 Acknowledgements

Part of this research has been funded by the Funds for Creative Research Groups of China (Grant No. 41521002), the National Science Fund for Outstanding Young Scholars of China (Grant No. 41622206), the International Cooperation Grant (NSFCRCUK_NERC) Resilience to Earthquake-induced landslide risk in China (41661134010), the National Key R & D Program of China (grant no. 2017YFC1501002), and the Fund of SKLGP (SKLGP2016Z002). David Sear and Wang Hao (respectively) are thanked for provision of the unpublished river flood and the Yigong dambreak flood grain-size data depicted in Fig. 1. Christoph Tuitz is thanked for the provision of the data plotted within Fig. 3. Jonathan Carrivick and Jim O'Connor are thanked for their careful insightful reviews of the manuscript that led to improved presentation of the arguments.

6.0 Author contributions

Carling conceptualized the approach, secured data and performed the analyses. Fan provided project funds, facilities and project administration during a Visiting Professorship for PAC at Chengdu University of Technology in 2019. PAC drafted the original manuscript and both authors engaged in review of text and figures in the final manuscript.

7.0 References

J. Adams, Wear of unsound pebbles in river headwaters, *Science*, **203**, 171-172 (1979).

J.R.L. Allen, Sedimentary Structures Their Character and Physical Basis, Volume I. Elsevier, Orford (1982).

L.A. Amy, P.J. Talling, V.O. Edmonds, E.J. Sumner, A. Lesueur, A., An experimental investigation of sand-mud suspension settling behaviour: implications for bimodal mud contents of submarine flow deposits. *Sedimentology*, **53**, 1411–1434 (2006).

E.D. Andrews, 1983. Entrainment of gravel from naturally sorted river-bed material. *Geological Society of America Bulletin*, **94**, 1225–1231 (1983).

M. Attal, J. Lavé, Pebble abrasion during fluvial transport: Experimental results and implications for the evolution of the sediment load along rivers. *Journal of Geophysical Research*, **114**, doi:10.1029/2009JF001328 (2009).

L. G. Austin, A treatment of impact breakage of particles. *Powder Technology*, **126**, 85–90 (2002).

V.R. Baker, "Discovering Earth's future in it past: palaeohydrology and global environmental change" in Global Continental Changes, Geological Society Special Publications **115**, J. Branson, A.G. Brown, K.J. Gregory, Eds. (Geological Society, 1996), pp. 73-83.

V.R. Baker, "High-energy megafloods: Planetary settings and sedimentary dynamics" in Flood and Megaflood Deposits: Recent and Ancient Examples, International Association of Sedimentologist Special Publication **32,** I.P. Martini, V.R. Baker, G. Garzon, Eds., (IAS, 2002), pp. 3-15.

V.R. Baker, The Channeled Scabland: A Retrospective. *Annual Reviews of Earth and Planetary Sciences*, **37**, 6.1-6.19 (2009).

V.R. Baker, P.A. Carling, Global Late Quaternary Megafloods, in Shroder, J. (Editor in Chief), Wohl, E.E. (Ed.), Treatise on Geomorphology, 2nd Edition, Vol. 9, Fluvial Geomorphology: Elsevier (2020 in press).

V.R. Baker, J.E. Costa, Flood power. In Catastrophic Flooding, eds. L. Mayer and D. Nash. Allen & Unwin, Boston, 1-21 (1987).

Ball, B.W. Payne, The tensile fracture of quartz crystals, *Journal of Materials Science*, **11,** 731–740 (1976).

G. Benito, Energy expenditure and geomorphic work of the cataclysmic Missoula flooding in the Columbia River Gorge, USA. *Earth Surface Processes and Landforms*, **22**, 457-472 (1997).

G. Benito, V. Thorndycraft, Catastrophic glacial-lake outburst flooding of the Patagonian Ice Sheet. *Earth-Science Reviews*, 102996 (2019).

T.C. Blair, J.G. McPherson, Grain-size and textural classification of coarse sedimentary particles. *Journal of Sedimentary Research*, **69**, 6–19 (1999).

A.C. Brayshaw, Bed microtopography and entrainment thresholds in gravel-bed rivers. Geological Society of America Bulletin 96, 218–223 (1985).

Z.T. Bieniawaski, The point-load test in geotechnical practice. *Engineering Geology*, **9**, 1-11 (1975).

W.C. Bradley, Effect of weathering on abrasion of granitic gravel, Colorado River (Texas). *Geological Society of America Bulletin*, **81**, 61-80 (1970).

W.C. Bradley, A.I. Mears, Calculations of flows needed to transport coarse fraction of Boulder Creek alluvium at Boulder, Colorado: summary. *Geological Society of America Bulletin*, **91**, 135–138 (1980).

J H. Bretz, Valley deposits immediately east of the channeled scabland of Washington. *Journal of Geology,* **37**, 505-541 (1929).

British Standard Institution, Code of practice for site investigations, BS 5930 HMSO, London (1981).

D.H. Campbell, Percussion marks on quartz grains. *Journal of Sedimentary Petrology*, **33**, 855-859 (1963).

P.A. Carling, Threshold of coarse sediment transport in broad and narrow natural streams. *Earth Surface Processes and Landforms*, **8**, 1-18 (1983).

P.A. Carling, Freshwater megaflood sedimentation: What can we learn about generic processes? *Earth-Science Reviews*, **125**, 87–113 (2013a).

P.A. Carling, Subaqueous "yardangs": Analogs for aeolian yardang evolution. *Journal of Geophysical Research: Earth Surface*, **118**, 276–287 (2013b).

P.A. Carling, M. Hoffmann, A.S. Blatter, "Initial motion of boulders in bedrock channels" in Ancient Floods, Modern Hazards: Principles and Applications of Paleoflood Hydrology, Water Science and Applications, 5, P. K. House, R. H. Webb, V. R. Baker, D. R. Levish, Eds. (American Geophysical Union, 2002), pp. 147-160.

P.A. Carling, K.J. Tinkler, "Conditions for entrainment of cuboid boulders in bedrock streams: an historical review of literature with respect to recent investigations" in Rivers over Rock: Fluvial Processes in bedrock Channels, K. J. Tinkler, E.E. Wohl, Eds. (American Geophysical Union, 1998), pp. 19-34.

P.A. Carling, D.M. Burr, T.F. Johnsen, T.A. Brennand, "A review of open-channel megaflood depositional landforms on Earth and Mars" in Megaflooding on Earth and Mars, D.M. Burr, P.A. Carling, V.R. Baker, Eds. (Cambridge University Press, 2009), pp. 33-49.

P.A. Carling, I. Villanueva, J. Herget, N. Wright, P. Borodavko, H. Morvan, Unsteady 1D and 2D hydraulic models with ice-dam break for Quaternary megaflood, Altai Mountains, southern Siberia. *Global and Planetary Change*, **70**, 24–34 (2010).

J.L. Carrivick, Modelling coupled hydraulics and sediment transport of a high-magnitude flood and associated landscape change. *Annals of Glaciology*, **45**, 143-154 (2007).

J.L. Carrivick, R. Jones, G. Keevil, Experimental insights on geomorphological processes within dam break outburst floods. *Journal of Hydrology*, **408**, 153-163 (2011).

J.L. Carrivick, J.K.P. Pringle, A.J. Russell, N.J. Cassidy, GPR-derived sedimentary architecture and stratigraphy of outburst flood sedimentation within a bedrock valley system, Hraundalur, Iceland. *Journal of Environmental and Engineering Geology*, **12**, 127-143 (2007).

J.L. Carrivick, A.J. Russell, F.S. Tweed, Geomorphological evidence for jökulhlaups from Kverkfjöll volcano, Iceland. *Geomorphology*, **63**, 81-102 (2004a).

J.I. Carrivick, A.J. Russell, F.S. Tweed, D. Twigg, Palaeohydrology and sedimentary impacts of jökulhlaups from Kverkfjöll, Iceland. *Sedimentary Geology*, **172**, 19-40 (2004b).

J.L. Carrivick, A.G. Turner, A.J Russell,T. Ingeman-Nielsen, J.C. Yde, Outburst flood evolution at Russell Glacier, western Greenland: effects of a bedrock channel cascade with intermediary lakes. *Quaternary Science Reviews*, **67**, 39-58 (2013).

J.L. Carrivick, F.S. Tweed, A review of glacier outburst floods in Iceland and Greenland with a megafloods perspective. *Earth-Science Reviews*, **196**, https://doi.org/10.1016/j.earscirev.2019.102876

T. Chelidze, T. Reuschle, Y. Gueguen, A theoretical investigation of the fracture energy of heterogeneous brittle materials. *Journal of Physics; Condensed Matter*, **6,** 1957–1868 (1994).

Z.X. Chen, C.J. Lim, J.R. Grace, Study of limestone particle impact attrition. *Chemical Engineering Science*, **62**, 867–877 (2007).

R.C. Chiverrell, D.A. Sear, J. Warburton, N. Macdonald, D. N. Schillereff, J.A. Dearing, I.W. Croudace, J. Brown, J. Bradley, Using lake sediment archives to improve understanding of flood magnitude and frequency: recent extreme flooding in northwest UK. *Earth Surface Processes and Landforms*, https://doi.org/10.1002/esp.4650, (17 May 2019).

H. Cho, L.G. Austin, An equation for the breakage of particles under impact. *Powder Technology*, **132**, 161–166 (2003).

M. Church, "Palaeohydrological reconstructions for a Holocene valley fill" in Fluvial Sedimentology. Canadian Society of Petroleum Geologists Memoir, **5**, A.D. Miall, ed. (Canadian Society of Petroleum Geologists, 1978), pp. 743–772.

J.E. Costa, Paleohydraulic reconstruction of flash-flood peaks from boulder deposits in the Colorado Front Range. *Geological Society of America Bulletin*, **94**, 986-1004 (1983).

J.E. Costa, J.E. O'Connor, "Geomorphically effective floods" in Natural and Anthropogenic Influences in Fluvial Geomorphology. Geophysical Monograph 89, J.E. Costa, Ed. (American Geophysical Union, 1995), pp. 45–56.

P.M. Cutler, P.M., Colgan, D.M., Mickelson, Sedimentologic evidence for outburst floods from the Laurentide Ice Sheet margin in Wisconsin, USA: implications for tunnel-channel formation. *Quaternary International***, 90**, 23–40 (2002).

G. Dam, Sedimentology of magmatically and structurally controlled outburst valleys along rifted volcanic margins: examples from the Nuussuaq Basin, West Greenland. *Sedimentology*, **49**, 505–532 (2002).

E.C. Dapples, J.F. Rominger, Orientation analysis of fine-grained clastic sediments: a report of progress. *The Journal of Geology*, **53**, 246-261 (1945).

S.E. Darby, H.Q. Trieu, P.A. Carling, J. Sarkkula, J. Koponen, M. Kummu, I. Conlan, J. Leyland, A physically based model to predict hydraulic erosion of fine-grained riverbanks: the role of form roughness in limiting erosion. *Journal of Geophysical Research*, **115**, F04003.

https://doi.org/10.1029/2010JF001708 (2010).

R.P. Denlinger, D.R.H. O'Connell, Simulations of cataclysmic outburst floods from Pleistocene Glacial Lake Missoula. *GSA Bulletin*, **122**, 678–689 (2010).

S. Dey, S.K.Z. Ali, Bed sediment entrainment by streamflow: State of the science. *Sedimentology*, **66**, 1449-1485 (2019).

R.K. Fahnestock, Morphology and hydrology of a glacial stream — White River, Mount Rainier, Washington. *US Geological Survey Professional Paper*, **422A**, 1–70 (1963).

J.D. Fenton, J.E. Abbott, Initial movement of grains on a stream bed: the effect of relative protrusion. *Proceedings of the Royal Society of London*, **A 352**, 523–537 (1977).

S. Foerster, M. Louge, H. Chang, K. Allia, Measurements of the collision properties of small spheres. *Physics of Fluids*, **6**, 1108-1115 (1994).

M. Fort, E. Cossart, G. Arnaud-Fassetta, 2010. Hillslope-channel coupling in the Nepal Himalayas and threat to man-made structures: The middle Kali Gandaki valley. *Geomorphology*, **124**, 178–199 (2010).

J.A. Franklin, International Society of Rock Mechanics Commission on Testing Methods. Suggested method for determining point load strength. *International Journal of Rock Mechanics and Mining Science and Geomechanics Abstracts*, **22**, 51-60 (1985).

M. Friedman, J. Handin, G. Alani, Fracture-surface energy of rock. *International Journal of Rock Mechanics and Mining Sciences*, **9,** 757–764 (1972).

O. Genc, A.H. Benzer, Single particle impact breakage characteristics of clinkers related to mineral composition and grindability. *Minerals Engineering*, **22**, 1160–1165 (2009).

C. Garcia, J.B. Laronne, M. Sala, Continuous monitoring of bed load flux in a mountain gravel-bed river. *Geomorphology* **34**, 23–31 (2000).

M. Ghadiri, Z. Zhang, Impact attrition of particulate solids. Part 1: a theoretical model of chipping. *Chemical Engineering Science*, **57**, 3659–3669 (2002).

A. Gupta, D.S. Yan, Mineral Processing Design and Operations. Elsevier, Amsterdam, 694pp (2016).

F.D.C. Hammond, A.D. Heathershaw, D.N. Langhorne, A comparison between Shields' threshold criterion and the movement of loosely packed gravel in a tidal channel. *Sedimentology*, **31**, 51–62 (1984).

B.O. Hardin, (1985) Crushing of soil particles. *Journal of Geotechnical Engineering*, ASCE, **111**, 1177–92 (1985).

A.B. Hawkins, Aspects of rock strength. *Bulletin of Engineering Geology and the Environment*, **57**, 17 – 30 (1998).

M. Heidari, G. Khanlari, M. Tobari Kaceh, S. Kargarian, Predicting the uniaxial compressive and tensile strengths of gypsum rock by point load testing. *Rock Mechanics and Rock Engineering*, **45**, 265-273 (2012).

Y. Hiramatsu, Y. Oka, Determination of the tensile strength of rock by a compression test of an irregular test piece. *International Journal of Rock Mechanics and Mining Sciences*, **3**, 89–90 (1966).

F. Hjulström, Studies in the morphological activity of rivers as illustrated by the River Fyris. *Bulletin of the Geological Institute University of Uppsala*, **25**, 221-527 (1935).

E. Hoek, E.T. Brown, Underground Excavations in Rock. Institution of Mining and Metallurgy, London, (1980).

R.T. Hukki, Proposal for a solomonic settlement between the theories of von Rittinger, Kick, and Bond. *Advances in Mechanical Engineering*, **223**, 403–408 (1962).

R.C. Hurley, J. Lind, D.C. Pagan, M.C. Akin, E.B. Herbold, In situ grain fracture mechanics during uniaxial compaction of granular solids. *Journal of Mechanics and Physics of Solids*, **112**, 273–90 (2018).

S.V. Izbash, S.V., Construction of Dams by Dumping Stones into Flowing Water. Translated 1935, Engineering Office, War Department, United States Engineer Office, Engineering Division, Eastport. Maine, USA, 138pp (1932).

S.V. Izbash, K.Y. Khaldre, Hydraulics of River Channel Closure. Butterworths (1970).

S. Kahraman, O. Gunaydin, M. Fener, The effect of porosity on the relation between uniaxial compressive strength and point load index. *International Journal of Rock Mechanics and Mining Sciences*, **42**, 584–589 (2005).

S.J. Kim. An Experimental Investigation of the Effect of Blasting on the Impact Breakage of Rocks. Unpubl. MSc thesis, Queen's University, Kingston, Ontario, Canada, 312pp (2010).

Y. Kodama, Downstream changes in the lithology and grain-size of fluvial gravels, the Watarase River, Japan: Evidence of the role of downstream fining. *Journal of Sedimentary Research*, **64A**, 68– 75 (1994a).

Y. Kodama, Experimental study of abrasion and its role in producing downstream fining in gravel-bed rivers. *Journal of Sedimentary Research*, **64A**, 76–85 (1994b).

P.D. Komar, Selective gravel entrainment and the empirical evaluation of flow competence. *Sedimentology*, **34**, 1165-1176 (1987).

P.D. Komar, P.A. Carling, Grain sorting in gravel-bed streams and the choice of particle sizes for flow competence evaluations. *Sedimentology*, **38**, 489–502 (1991).

E.H. Koster, B.R. Rust, D.J. Gendzwil, The ellipsoidal form of clasts with practical applications to fabric and size analyses of fluvial gravels. *Canadian Journal of Earth Sciences*, **17**, 1725-1739 (1980).

V.M. Kuznetsov, The mean diameter of the fragments formed by blasting rock. *Soviet Mining Science*, **9**, 144-148 (1973).

L. Labous, A.D. Rosato, R.N. Dave, Measurements of collisional properties of spheres using high-speed video analysis. *Physical Review E*, **56**, 5717-5725 (1997).

P.V. Lade, J.A. Yamamuro, P.A. Bopp, P.A., ignificance of particle crushing in granular materials—Closure. *Journal of Geotechnical and Geoenvironmental Engineering*, ASCE, **123**, 889–90 (1996).

M. P. Lamb, N.J. Finnegan, J.S. Scheingross, L.S. Sklar, New insights into the mechanics of fluvial bedrock erosion through flume experiments and theory. *Geomorphology*, **244**, 33-55. (2015).

K.R. Langmaak, Initial Motion of Riprap on Steep Slopes. Unpublished MSC thesis, Stellenbosch University, Stellenbosch, South Africa, 153pp (2013).

K.R. Langmaak, G.R. Basson, Incipient motion of riprap on steep slopes. *Journal of Hydraulic Engineering*, **141**, 06015010 (2005).

J.B. Laronne, I. Reid, Y. Yitshak, L.E. Frostick, The non-layering of gravel streambeds under ephemeral flood regimes. *Journal of Hydrology*, **159**, 353-363 (1994).

J. de Leeuw, J., M.P. Lamb, G. Parker, A. Moodie, D. Haught, J.G. Venditti, J.A. Nittrouer, Entrainment and suspension of sand and gravel. *Earth Surface Dynamics: Discussions*, https://doi.org/10.5194/esurf-2019-67 (2019).

W.L. Lim, G.R. McDowell, A.C. Collop, The application of Weibull statistics to the strength of railway ballast. *Granular Matter*, **6**, 229–37 (2004).

I. Lønne, Facies characteristics of a proglacial turbidite sand-lobe at Svalbard. *Sedimentary Geology*, **109**, 13–35 (1997).

L.M. Lord, A.E. Kehew, Sedimentology and paleohydrology of glacial-lake outburst deposits in southeastern Saskatchewan and northwestern North Dakota. *Geological Society of America Bulletin,* **99**, 663–673 (1987).

J.K. Maizels, J.K., Lithofacies variations within sandur deposits: the role of runoff regime, flow dynamics and sediment supply characteristics. *Sedimentary Geology*, **85**, 299–325 (1993).

H.E. Malde, The catastrophic late Pleistocene Bonneville Flood in the Snake River Plain, Idaho. US Geological Survey Professional Paper 596, 52pp.

P.A. Mantz, Incipient transport of fine grains and flakes by fluids – extended Shields diagram. *Journal of the Hydraulics Division, ASCE*, **103**, 601–615 (1977).

P.M. Marren, Magnitude and frequency in proglacial rivers: a geomorphological and sedimentological perspective. *Earth-Science Reviews*, **70**, 203-251 (2005).

A.J. Moss, Technique for assessment of particle breakage in natural and artificial environments. *Journal of Sedimentary Petrology*, **42**, 725–8 (1972).

E. Mutti, G. Davoli, R. Tinterri, C. Zavala, The importance of ancient fluviodeltaic systems dominated by catastrophic flooding in tectonically active basins. *Memoire di Scienze Geologiche*, **48**, 233–291 (1996).

S.L. Norris, M. Margold, G.J. Utting, D.G. Froese, Geomorphic, sedimentary and hydraulic reconstruction of a glacial lake outburst flood in northern Alberta, Canada. *Boreas*. https://doi.org/10.1111/bor.12403. ISSN 0300-9483 (2019).

J.E. O'Connor, Hydrology, Hydraulics, and Geomorphology of the Bonneville Flood. GSA Special Paper 274, 83pp (1993).

F. Ouchterlony, Review of fracture toughness testing of rock, *SM Archives*, **7,** 131–211 (1982).

T. Pähtz, O. Durán, The cessation threshold of nonsuspended sediment transport across aeolian and fluvial environments. *Journal of Geophysical Research: Earth Surface*, **123,** 1638–1666 (2018).

F. Papp, "Extremeness of extreme floods" in The Extreme of the Extremes: Extraordinary Floods, IAHS Special Publication, 271, Á. Snorasson, H.P. Finnsdóttir, M. Moss, Eds. (IAHS, 2002), pp. 373-378.

E. Petrakis, E. Stamboliadis, K. Komnitsas, Evaluation of the relationship between energy input and particle size distribution in comminution with the use of piecewise regression analysis, *Particulate Science and Technology*, **35**: 479-489 (2017).

E.D. Pittman, A.T. Ovenshine, Pebble morphology in the Merced River (California). *Sedimentary Geology*, **2**, 125-140 (1968).

D.M. Powell, P.J. Ashworth, Spatial pattern of flow competence and bed-load transport in a divided gravel-bed river. *Water Resources Research,* **31**, 741–752 (1995).

M. Ramette, A. Heuzel, Le Rhône à Lyon: étude de l'entraînement des galets à l'aide de traceurs radioactifs. *La Houille Blanche*, **No. Spécial A**, 389-394 (1962).

K. Richardson, I. Benson, P.A. Carling, "An instrument to record sediment movement in bedrock channels" in Erosion and Sediment Transport Measurement in Rivers: Technological and Methodological Advances, IAHS Publ. 283, I. Bogen, T. Fergus, D. E. Walling, Eds, 228-235 (2003).

K. Richardson and P.A. Carling, A typology of sculpted forms in open bedrock channels. *The Geological Society of America, Special Paper*, **392**, 108pp (2005).

A.J. Russell, Catastrophic floods. In: Selby, R.C., Cocks, L.R.M., Primer, I.R. (Eds.), Encylopedia of Geology. Elsevier, Oxford, pp. 628-641 (2005).

A.J. Russell, Ó. Knudsen, Ancient-contact rhythmite (turbidite) succession deposited during the November 1996 catastrophic outburst flood (jökulhlaup), Skeiðarárjökull, Iceland. *Sedimentary Geology*, **127**, 1–10 (1999).

A.J. Russell, P.M. Marren, Proglacial fluvial sedimentary sequences in Greenland and Iceland: a case study from active proglacial environments subject to jökulhlaups. In: Jones, A.P., Tucker, M.E., Hart, J.K. (Eds.), QRA Technical Guide Number 7, London, pp. 171–208 (1999).

B.R. Rust, Pebble orientation in fluvial sediments. *Journal of Sedimentary Petrology*, **42**, 384-388 (1972).

B.R. Rust, Depositional model for braided alluvium. In: Fluvial Sedimentology, Memoir **5**, 605-625 (1977).

S. M. Sadat-Helbar, E. Amiri-Tokaldany, S. E. Darby, A. Shafaie, Fall velocity of sediment particles. Proceedings of the 4th IASME/WSEAS International Conference on Water Resources, Hydraulics and Hydrology (WHH'09), 39-45 (2009).

Schendel, N. Goseberg, T. Schlurmann, Erosion of wide-graded quarry-stone material under unidirectional current. *Journal of Waterway, Port, Coastal and Ocean Engineering*, DOI: 10.1061/(ASCE)WW.1943-5460.0000321 (2014).

H. Schlichting, K. Gersten, Boundary Layer Theory, 8th Edition, Springer-Verlag, Berlin Heidelberg (2000).

O.E. Sequeiros, B. Spinewine, R.T. Beaubouef, T. Sun, M.H. Garcia, M.H., P. Parker, Bedload transport and bed resistance associated with density and turbidity currents. *Sedimentology*, **57**, 1463–1490 (2010).

Y. Shang, Z. Yang, L. Li, D.A. Liu, Q. Liao, Y. Wang, A super-large landslide in Tibet in 2000: background, occurrence, disaster, and origin. *Geomorphology*, **54**, 225-243 (2003).

G. Shanmugam, The Bouma sequence and the turbidite mind set. *Earth-Science Reviews*, **42**, 201-229 (1997).

T.N. Singh, A. Kainhola, A. Venkatesh, Correlation between point load index and uniaxial compressive strength for different rock types. *Rock Mechanics and Rock Engineering,* **45**, 259–264 (2012).

W.J. Stronge, Impact Mechanics. Cambridge University Press, Cambridge, 280pp (2000).

A.Sundborg, The River Klaralven; a study of fluvial processes. *Geografiska Annaler*, **38**, 125-316 (1956).

L.M. Tavares, R.P. King, Single-particle fracture under impact loading. *International Journal of Mineral Processing*, **54**, 1–28 (1998).

Tómasson, H., 2002. Catastrophic Floods in Iceland. In: Snorrason, A., Finnsdóttir, H.P., Moss, M. (Eds.), The Extremes of the Extremes: Extraordinary Floods. IAHS, Wallingford, pp. 121-126.

C. Tuitz, U. Exner, M. Frehner, B. Grasemann, The impact of ellipsoidal particle shape on pebble breakage in gravel. *International Journal of Rock Mechanics and Mining Sciences*, **54**, 70-79 (2012).

E.T. Tuzcu, R.K. Rajamani, Modeling breakage rates in mills with impact energy spectra and ultra-fast load cell data. *Minerals Engineering*, **24**, 252–260 (2011).

G.A. Valentine, Stratified flow in pyroclastic surges. *Bulletin of Volcanology*, **50**, 352-355 (1987).

L.C. van Rijn, Critical movement of large rocks in currents and waves. International Journal of Sediment Research, **34**, 387-398 (2019).

W.H. Walker, W.K. Lewis, W.H. McAdams, E.R. Gilliland, Principles of Chemical Engineering. McGraw-Hill, NY, USA (1937).

K.X. Whipple, G.S. Hancock, R.S. Anderson, River incision into bedrock: Mechanics and relative efficacy of plucking, abrasion, and cavitation. *Geological Society of America, Bulletin,* **112**, 490–503 (2000).

G.P. Williams, Paleohydrological methods and some examples from Swedish fluvial environments, I– Cobble and boulder deposits. *Geografiska Annaler*, **65A**, 227-243 (1983).

B.A. Wills, T.J. Napier-Munn, Will's Mineral Processing, 7th Edition, Elsevier (2006).

J. Winsemann, J. Lang, "Flooding Northern Germany: Impacts and Magnitudes of Middle Pleistocene Glacial-Lake-Outburst Floods" in Palaeohydrology, J. Herget, A. Fontana, Eds. (Springer, 2020), pp. 29-47.

K.H. Wohletz, M.F. Sheridan, W.K. Brown, Particle size distributions and the sequential fragmentation/transport theory applied to volcanic ash. *Journal of Geophysical Research*, **94**, 703-721 (1999).

M.G. Wolman, J.P. Eiler, Reconnaissance study of erosion and deposition produced by the flood of August 1955 in Connecticut. *Transactions of the American Geophysical Union*, **39**, 1–14 (1958).

Y. Xu, Y. Wang, Size effect on specific energy distribution in particle comminution. *Fractals*, **25**, 1750016 (2017).

Conflict of Interest Statement

The authors note no conflicting interests.